p21 delays tumor onset by preservation of chromosomal stability

Juan A. Barboza*†, Geng Liu*, Zhenlin Ju*‡, Adel K. El-Naggar§, and Guillermina Lozano*†¶

Departments of *Cancer Genetics and §Pathology, University of Texas M. D. Anderson Cancer Center, 1515 Holcombe Boulevard, Houston, TX 77030; and †Graduate School of Biomedical Sciences, University of Texas, Houston, TX 77030

Edited by Arnold J. Levine, Institute for Advanced Study, Princeton, NJ, and approved November 2, 2006 (received for review July 25, 2006)

The p53 protein suppresses tumorigenesis by initiating cellular functions such as cell cycle arrest and apoptosis in response to DNA damage. A p53 mutant, p53R172P, which is deficient for apoptosis but retains a partial cell cycle arrest function, delays tumor onset in mice. Remarkably, lymphomas arising in *Trp53*$^{515C/515C}$ mice (encoding p53R172P) retain stable genomes. Given the dominant role of p21 in p53 cell cycle control, we crossed *Trp53*$^{515C/515C}$ mice onto a *p21*-null background to determine whether p21 was required for maintaining chromosomal stability and delaying tumor onset. Loss of *p21* completely abolished the cell cycle arrest function of p53R172P and accelerated tumor onset in *Trp53*$^{515C/515C}$ mice. Cytogenetic examination of *Trp53*$^{515C/515C}$ *p21*$^{-/-}$ sarcomas and lymphomas revealed aneuploidy and chromosomal aberrations that were absent in *Trp53*$^{515C/515C}$ malignancies. Thus, p21 coupled p53-dependent checkpoint control and preservation of chromosomal stability, and cooperated with apoptosis in suppressing tumor onset in mice.

apoptosis | chromosomal instability | p53 | tumorigenesis | mouse model

The role of p53 in tumor suppression is well established. Transcriptional activation of a large repertoire of target genes implicates p53 in tumor-preventive functions, such as cell cycle control, apoptosis, and maintenance of chromosomal stability. Control of the cell cycle by p53 is primarily accomplished by activation of the cyclin-dependent kinase inhibitor, p21, resulting in a G_1 arrest after DNA damage (1, 2). Loss of *p21* severely compromises the G_1 checkpoint control by p53 (3–5). However, *p21*$^{-/-}$ mice are resistant to early onset tumorigenesis (3, 6–8). Similarly, deletion of *Gadd45*, a p53 target gene involved in the G_2/M progression, causes centrosome amplification and chromosomal instability (CIN) but does not predispose mice to tumorigenesis (9). These findings reveal the importance of proper cell cycle control in maintaining genomic integrity and suggest that cell cycle control plays a redundant role with other p53 functions in suppressing tumorigenesis.

Deletion of the p53 apoptotic targets, *Noxa*, *Puma*, and *Bax*, in mice also has demonstrated their dispensable role in preventing early tumor onset (10–13). To better address the role of p53-dependent cell cycle control and apoptosis in tumor suppression, we exploited the properties of a rare apoptosis-deficient human p53 Arg-to-Pro mutant, p53R175P, which retains a cell cycle arrest function (14, 15). *Trp53*$^{515C/515C}$ mice (encoding p53R172P, the corresponding murine mutant) are deficient for apoptosis but retain a partial cell cycle arrest function and have a prolonged survival compared with *Trp53*$^{-/-}$ mice (16). Importantly, *Trp53*$^{515C/515C}$ lymphomas that develop late have stable genomes unlike *Trp53*$^{-/-}$ malignancies, which are characterized by CIN (16, 17). These data demonstrate that p53-dependent apoptosis is not solely responsible for preventing tumor onset and suggest that p53 cell cycle control may suppress tumorigenesis by preservation of genomic integrity.

Given the dominant role of p21 in p53 cell cycle control, we generated double mutant mice, *Trp53*$^{515C/515C}$*p21*$^{-/-}$, to test whether loss of proper cell cycle control via p21 resulted in CIN, enhancing tumor onset in *Trp53*$^{515C/515C}$ mice. Here, we demonstrate that p21 cell cycle control cooperates with the apoptotic pathway for effective tumor suppression by p53. Our results explain the failure of mouse models with deletion of individual p53 target genes to recapitulate a *Trp53*-null tumor phenotype (18). Thus, combination therapies targeting p53 cell cycle and apoptotic pathways are crucial for tumor suppression.

Results

In response to DNA damage, p21 activation by p53 is essential in mediating a cell cycle arrest (3–5). To assay p53R172P induction of p21, *Trp53*$^{515C/515C}$ mouse embryo fibroblasts (MEFs) were exposed to DNA damage, and p21 levels were examined by immunoblot analysis. Like wild-type p53, p53R172P was stabilized after γ-radiation and induced the expression of p21 (Fig. 1*A*). Under the same conditions, p21 protein was not detected in *Trp53*$^{-/-}$ or *Trp53*$^{515C/515C}$*p21*$^{-/-}$ cells. We next addressed the importance of p21 in response to p53R172P by examining the cell cycle progression of *Trp53*$^{515C/515C}$*p21*$^{-/-}$ and *Trp53*$^{515C/515C}$ MEFs. Subconfluent cultures of early passage MEFs were treated with γ-radiation then labeled with BrdU to determine the proportion of cells in S phase. *Trp53*$^{515C/515C}$ and *p21*$^{-/-}$ MEFs retained a partial p53-dependent cell cycle arrest, as evidenced by a reduction in the ratio of cells in S phase after irradiation compared with *Trp53*$^{-/-}$ cells (Fig. 1*B*). In contrast, the number of *Trp53*$^{-/-}$ and *Trp53*$^{515C/515C}$*p21*$^{-/-}$ MEFs in S phase was similar after treatment, indicating the absence of a cell cycle arrest in these cells. These findings indicate that p21 entirely mediated the cell cycle checkpoint control by p53R172P in response to γ-radiation.

To further explore the importance of p21 to cell cycle control in response to p53R172P, we analyzed the growth rates and saturation densities of early passage MEFs. At day 4 of culture, *Trp53*$^{515C/515C}$*p21*$^{-/-}$ and *Trp53*$^{-/-}$ cells continued proliferating and attained a higher saturation density than *Trp53*$^{515C/515C}$, wild-type, or *Trp53*$^{515C/+}$*p21*$^{-/-}$ cells (Fig. 1*C*). Thus, *p21* loss delayed the ability of p53R172P to arrest cell proliferation upon contact inhibition, resembling the *Trp53*-null phenotype. Taken together these data demonstrate the importance of p21 in mediating a p53-dependent cell cycle arrest.

Author contributions: J.A.B., G. Liu, and G. Lozano designed research; J.A.B., G. Liu, Z.J., and A.K.E.-N. performed research; J.A.B., G. Liu, Z.J., and A.K.E.-N. analyzed data; and J.A.B. wrote the paper.

The authors declare no conflict of interest.

This article is a PNAS direct submission.

Freely available online through the PNAS open access option.

Abbreviations: MEF, mouse embryo fibroblast; CIN, chromosomal instability.

Data deposition: The microarray data reported in this paper have been deposited in the ArrayExpress database (accession no. E-MEXP-917).

‡Present address: Department of Chemistry and Biochemistry, Texas State University, 601 University Drive, San Marcos, TX 78666.

¶To whom correspondence should be addressed at: University of Texas M. D. Anderson Cancer Center, 1515 Holcombe Boulevard, Unit 1010, Houston, TX 77030. E-mail: gglozano@mdanderson.org.

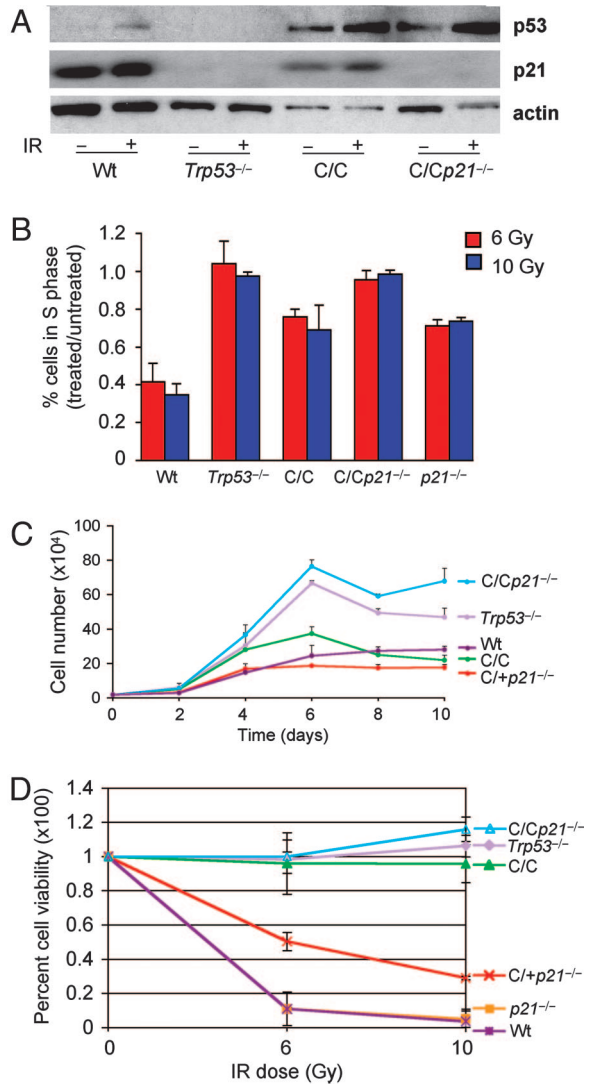

Fig. 1. *Trp53*$^{515C/515Cp21-/-}$ cells are deficient for apoptosis and cell cycle arrest. (*A*) Immunoblot analysis of p53 and p21 in MEFs of the indicated genotypes before and after treatment with 6 Gy of γ-radiation. Actin was used as a loading control. (*B*) Cell cycle progression was assayed by determining the ratio of cells in S phase from irradiated (6 Gy) to nonirradiated MEFs with different genotypes: wild-type (Wt), *Trp53*$^{-/-}$, *Trp53*$^{515C/515C}$ (C/C), *Trp53*$^{515C/515Cp21-/-}$ (C/C*p21*$^{-/-}$), and *p21*$^{-/-}$. (*C*) Equal numbers of MEFs of different genotypes at passage 2 were plated in triplicate and counted at the indicated times. Similar results were obtained from at least two independently derived MEF lines. (*D*) Apoptosis in mouse thymocytes after treatment with γ-radiation was measured by labeling cells with Annexin-V. Depicted are average values determined from at least three mice of each genotype with SE shown.

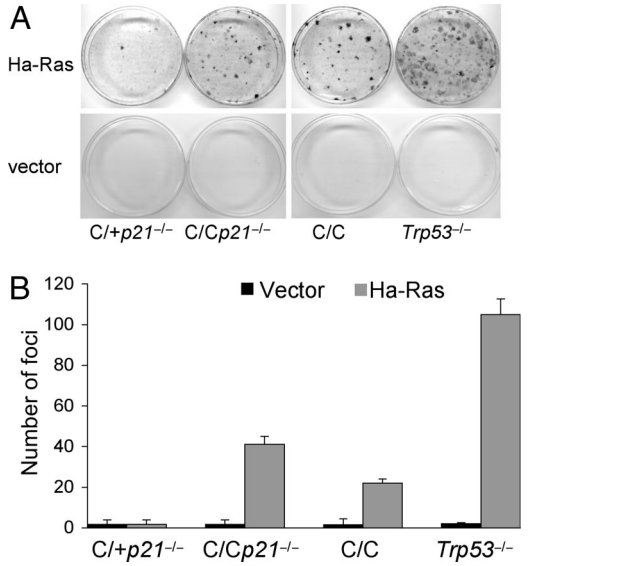

Fig. 2. Loss of *p21* enhances transformation of *Trp53*$^{515C/515C}$ MEFs by oncogenic *Ras*. (*A*) Transformation of *Trp53*$^{515C/+p21-/-}$ (C/+*p21*$^{-/-}$), *Trp53*$^{515C/515Cp21-/-}$ (C/C*p21*$^{-/-}$), *Trp53*$^{515C/515C}$ (C/C), and *Trp53*$^{-/-}$ MEFs in cooperation with activated *Ras* was determined by a focus-forming assay. Passage-2 cells were infected with an *Ha-Ras*^{V12} or control retroviral vector and plated with noninfected cells of the same genotype. Foci were counted after 15 days of culture. (*B*) Quantification of the number of foci arising in MEFs with different genotypes. Depicted are averages with SEs as determined from triplicate dishes from a representative experiment performed three times.

Murine thymocytes undergo p53-dependent apoptosis upon exposure to γ-radiation (19). By using this methodology, we have previously shown that p53R172P is completely deficient for apoptosis *in vivo* (16). In further characterization of *Trp53*$^{515C/515C}$*p21*$^{-/-}$ mice, freshly isolated thymocytes were treated with γ-radiation and stained with Annexin-V, a marker for apoptosis, to determine cell viability. *Trp53*$^{515C/515C}$, *Trp53*$^{515C/515C}$*p21*$^{-/-}$, and *Trp53*$^{-/-}$ thymocytes remained viable after treatment with 6 and 10 Gy of γ-radiation (Fig. 1*D*). In contrast, wild-type and *p21*$^{-/-}$ cells displayed abundant cell death, whereas *Trp53*$^{515C/+}$*p21*$^{-/-}$ cells displayed an intermediate viability. Thus, in response to γ-radiation, *Trp53*$^{515C/515C}$*p21*$^{-/-}$ cells, like *Trp53*$^{-/-}$ cells, were completely deficient for apoptosis and cell cycle arrest functions.

Trp53-deficient mouse fibroblasts bypass *Ras*-induced replicative senescence and undergo transformation (20). To begin to address the importance of p21 in tumor suppression in the absence of p53-dependent apoptosis, we assayed the focus-forming potential of early passage *Trp53*$^{515C/515C}$, *Trp53*$^{515C/515C}$*p21*$^{-/-}$, *Trp53*$^{515C/+}$*p21*$^{-/-}$, and *Trp53*$^{-/-}$ MEFs infected with a retroviral vector encoding an *Ha-Ras*^{V12} cDNA. *Trp53*$^{515C/515C}$ MEFs exhibited a transformation potential in response to activated *Ras*, forming ≈20% the number of foci as *Trp53*$^{-/-}$ cells (Fig. 2). Loss of *p21* enhanced transformation by oncogenic *Ras* as *Trp53*$^{515C/515C}$*p21*$^{-/-}$ cells formed ≈40% the number of foci as *Trp53*$^{-/-}$ cells. In contrast, few foci were formed by *Trp53*$^{515C/+}$*p21*$^{-/-}$ cells. Thus, the p53R172P mutant exhibited transformation potential in combination with oncogenic *Ras* that was enhanced by loss of *p21*. Yet, loss of *p21* alone in a wild-type p53 background did not affect transformation.

Because p53R172P is completely deficient for inducing apoptosis and loss of *p21* completely abolished its cell cycle arrest function, *Trp53*$^{515C/515C}$*p21*$^{-/-}$ mice were monitored for survival and tumor incidence. Deletion of *p21* significantly accelerated tumor incidence in *Trp53*$^{515C/515C}$ mice (Fig. 3*A*). The median survival of *Trp53*$^{515C/515C}$ mice was 395 days, whereas that of *Trp53*$^{515C/515C}$*p21*$^{-/-}$ mice was 233 days (P = 0.0001). *Trp53*$^{515C/515C}$*p21*$^{-/-}$ mice began to develop tumors at a rate similar to that of *Trp53*$^{-/-}$ mice, yet their overall survival was significantly prolonged (P = 0.001). Although 50% of *Trp53*$^{515C/515C}$*p21*$^{-/-}$ mice were tumor-bearing at 233 days, >80% of *Trp53*$^{-/-}$ mice had succumbed to tumorigenesis at this time point. The types of tumors arising in *Trp53*$^{515C/515C}$*p21*$^{-/-}$ mice resembled those of *Trp53*$^{515C/515C}$ and *Trp53*$^{-/-}$ mice being mainly composed of sarcomas and lymphomas (16, 21, 22). Consistent with previous data, 45% of *Trp53*$^{515C/515C}$ mice developed sarcomas, whereas 50% succumbed to lymphomas. In *Trp53*$^{515C/515C}$*p21*$^{-/-}$ mice, the incidence of sarcomas rose to 59%, and lymphomas were reduced to 31%. *Trp53*$^{515C/515C}$*p21*$^{-/-}$ animals developed different

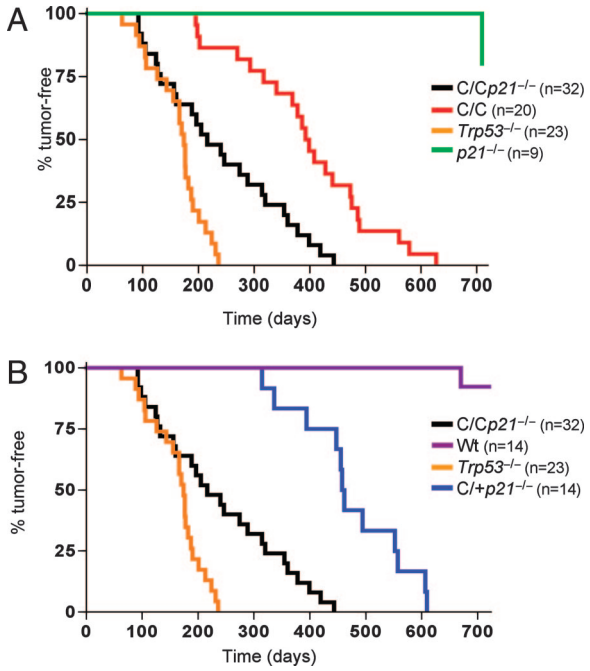

Fig. 3. Loss of *p21* accelerates tumor onset in $Trp53^{515C/515C}$ mice. Shown are tumor-free survival rates of $Trp53^{515C/515C}$ (C/C; $n = 20$), $Trp53^{515C/515Cp21-/-}$ (C/C$p21^{-/-}$; $n = 32$) $Trp53^{-/-}$ ($n = 23$), wild-type (Wt, $n = 14$), $p21^{-/-}$ ($n = 9$), and $Trp53^{515C/+p21-/-}$ (C/+$p21^{-/-}$; $n = 14$) mice. Survival was calculated by using the Kaplan–Meier method.

types of sarcomas, including angiosarcomas, spindle cell sarcomas, and anaphasic and biphasic sarcomas. Lymphomas were classified as diffuse and/or histiocytic. In addition, some $Trp53^{515C/515C}p21^{-/-}$ mice developed carcinomas (6%), and one had a benign adenoma (3%).

The strain of $p21^{-/-}$ mice used in this study are not tumor-prone likely because of an intact apoptotic response (5). Accordingly, $Trp53^{515C/+}p21^{-/-}$ mice, like $p21^{-/-}$ animals retaining a p53-dependent apoptotic response, had a prolonged survival rate compared with $Trp53^{515C/515C}p21^{-/-}$ mice that were deficient for apoptosis (Figs. 1*D* and 3*B*). These results indicate that p53-dependent apoptosis was essential for tumor suppression in the absence of *p21* and revealed a cooperative relationship between p21 expression and p53-dependent apoptosis in suppression of tumorigenesis.

Because $Trp53^{515C/515C}$ MEFs and tumor cells contain diploid genomes (16), we also addressed the role of p21 in maintaining chromosomal stability. Metaphase spreads of early passage $Trp53^{515C/515C}$, $Trp53^{515C/515C}p21^{-/-}$, and $Trp53^{-/-}$ MEFs were surveyed for chromosomal aberrations in the absence of DNA damage. As previously reported (16), $Trp53^{515C/515C}$ MEFs, like wild-type cells, contained few chromosomal aberrations (2.6% and 3.0%, respectively) (Fig. 4*A*). However, 13% of $Trp53^{515C/515C}p21^{-/-}$ and 25% of $Trp53^{-/-}$ MEFs harbored chromosomal abnormalities. Thus, p21 coupled cell cycle control and maintenance of chromosomal stability.

To probe for CIN in tumors, cells from lymphomas and sarcomas arising in $Trp53^{515C/515C}$ and $Trp53^{515C/515C}p21^{-/-}$ mice were also analyzed for chromosomal aberrations. Metaphase spreads of $Trp53^{515C/515C}$ sarcomas (three cases) and lymphomas (four cases) revealed a diploid chromosome content and few chromosomal aberrations as previously published for lymphomas (16) (Fig. 4 *B* and *C*). However, three of four sarcomas and five of seven lymphomas from $Trp53^{515C/515C}p21^{-/-}$ mice had aneuploid genomes with overt chromosomal aberrations such as breaks, fusions, and marker chromosomes. These aberrations

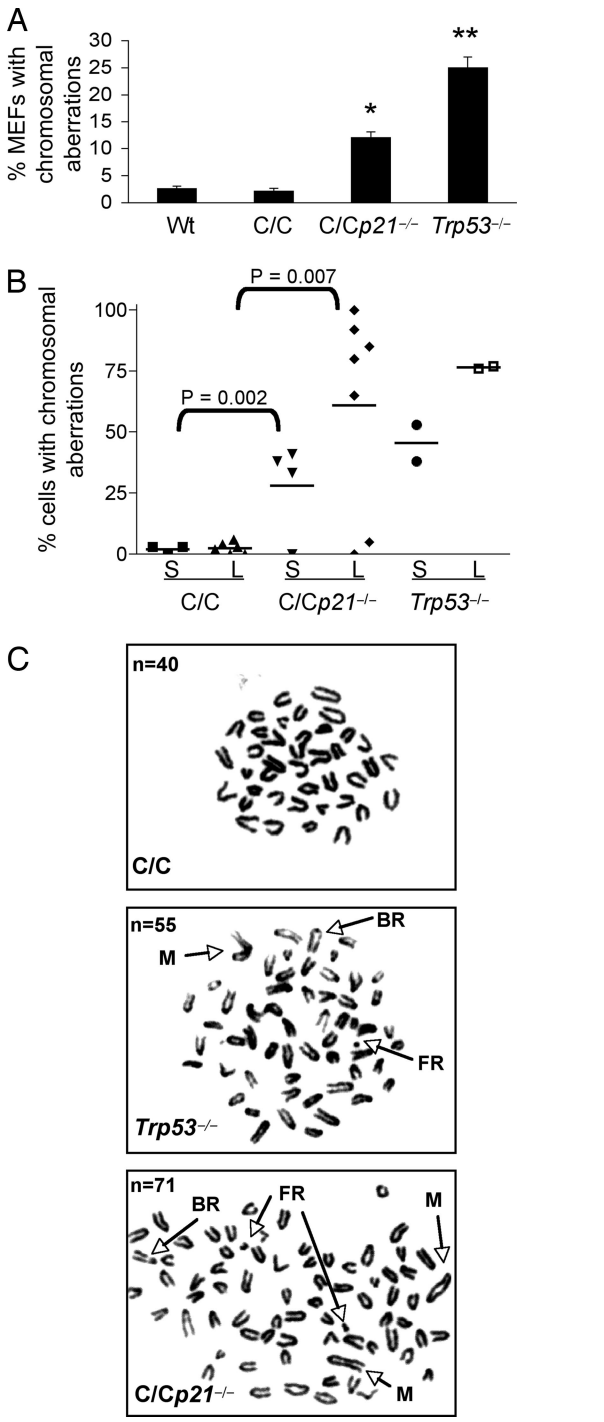

Fig. 4. Loss of *p21* causes CIN in $Trp53^{515C/515C}$ MEFs and tumors. (*A*) Metaphase spreads from wild-type (Wt), $Trp53^{515C/515C}$ (C/C), $Trp53^{515C/515Cp21-/-}$ (C/C$p21^{-/-}$), and $Trp53^{-/-}$ MEFs at passage 2 were scored for chromosomal aberrations ($n = 128$ metaphases scored). *, $P < 0.01$; **, $P < 0.005$ (Student's *t* test). (*B*) Percentage of sarcoma (S) or lymphoma (L) tumor cells with chromosomal aberrations arising in *p53* mutant mice. At least 30 cells per tumor sample were scored for chromosomal aberrations. *P* values were determined by Student's *t* test. (*C*) Representative metaphase spreads of lymphoma cells derived from *p53* mutant mice. FR, fragment; BR, break; M, marker. n, total chromosome number.

were similar to those in *Trp53*-null tumors. These results demonstrate that loss of p53-dependent apoptosis and p21 expression led to improper cell cycle control, development of CIN, and subsequent tumor development.

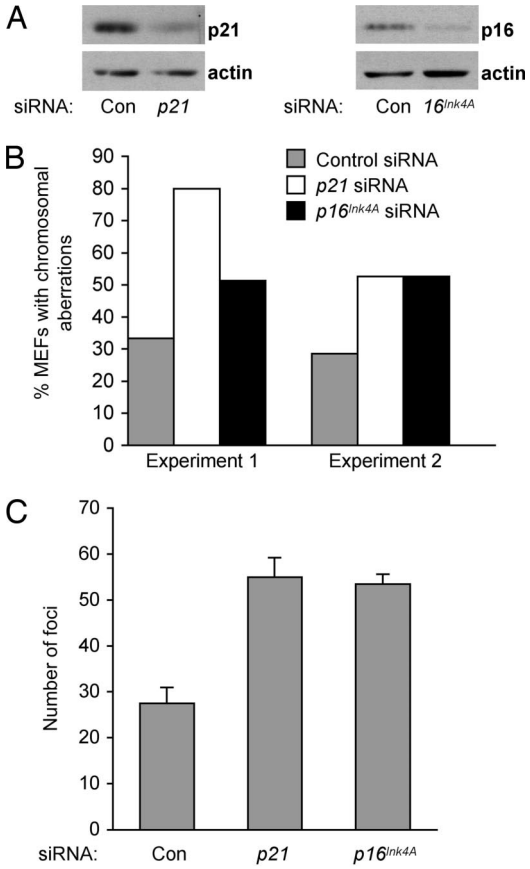

Fig. 5. *p16*^{Ink4A} deficiency enhanced CIN and transformation of *Trp53*$^{515C/515C}$ cells. (*A*) *Trp53*$^{515C/515C}$ MEFs at passage 2 were transfected with the indicated siRNAs, and decreased protein levels were confirmed by immunoblot analysis. (*B*) Metaphase spreads of *Trp53*$^{515C/515C}$ MEFs transfected with the indicated siRNAs were scored for chromosomal aberrations. Depicted are the results obtained from two independent experiments in which duplicate dishes of MEFs were transfected with siRNAs then pooled for chromosomal analysis 6 days later. (*C*) *Trp53*$^{515C/515C}$ MEFs were infected with *Ha-Ras*^{V12}, transfected with the indicated siRNAs, and then plated 48 h later. Foci were counted at day 15. Con, control.

We have shown that *p21* loss led to CIN and enhanced *Ras*-induced transformation of *Trp53*$^{515C/515C}$ MEFs. To determine whether these effects were specific to p21 or could be caused by disruption of other cell cycle regulators, we performed siRNA experiments to down-modulate *p16*^{Ink4A}, which encodes another cyclin-dependent kinase inhibitor that regulates the G_1/S transition (23, 24). Low passage *Trp53*$^{515C/515C}$ MEFs were transfected with control siRNA or siRNAs specific for *p21* or *p16*^{Ink4A}, and expression was confirmed by immunoblot analysis (Fig. 5*A*). To detect chromosomal alterations, cells were cultured for two additional passages after transfection with siRNAs and then prepared for chromosomal analysis. As with genetic ablation of *p21*, down-modulation of *p21* by siRNA increased the incidence of chromosomal aberrations in *Trp53*$^{515C/515C}$ MEFs by 2- to 3-fold over cells transfected with control siRNA (Fig. 5*B*). Transfection with *p16*^{Ink4A} siRNA also enhanced the abundance of cells with chromosomal aberrations approximately 2-fold over control cells. These results demonstrate that loss of *p16*^{Ink4A}, like loss of *p21*, was sufficient to disrupt chromosomal stability in *Trp53*$^{515C/515C}$ MEFs.

Because *p16*^{Ink4A} is commonly inactivated in human tumors (25), we sought to determine whether *p16*^{Ink4A} deficiency, like *p21* loss, would bestow oncogenic potential to *Trp53*$^{515C/515C}$ MEFs. To this end, we performed focus-forming assays with *Ha-Ras*^{V12}-infected *Trp53*$^{515C/515C}$ MEFs transfected with *p21*, *p16*^{Ink4A}, or control siRNAs. As in previous experiments, *p21* loss caused a 2-fold increase in the number of *Trp53*$^{515C/515C}$ foci formed compared with control cells (Fig. 5*C*). Similarly, cells transfected with *p16*^{Ink4A} siRNA also formed twice as many foci as did cells transfected with control siRNA. Thus, disruption of two critical cell cycle regulators permitted the development of CIN and increased transformation potential in the absence of p53-dependent apoptosis.

Although loss of *p21* accelerated tumor onset in *Trp53*$^{515C/515C}$ mice, the survival of *Trp53*$^{515C/515C}$*p21*$^{-/-}$ and *Trp53*-null mice was significantly different ($P = 0.001$) (Fig. 3). We therefore surveyed gene expression by microarray analysis in an attempt to identify additional p53R172P-dependent genes that may have conferred a survival advantage to *Trp53*$^{515C/515C}$*p21*$^{-/-}$ mice. Wild-type, *Trp53*$^{515C/515C}$, and *Trp53*-null MEFs were treated with γ-radiation and harvested 6 h after treatment. Gene expression profiles from irradiated wild-type and *Trp53*$^{515C/515C}$ MEFs were compared with profiles of irradiated *Trp53*-null MEFs. Twenty-nine and 18 genes were differentially expressed in wild-type and *Trp53*$^{515C/515C}$ MEFs, respectively, compared with *Trp53*-null MEFs according to the criteria detailed in *Materials and Methods*. Genes with a fold change ≥2 and previously characterized as p53 targets (26–30) or determined to have consensus p53 binding sites (31) are listed in Table 1. Three genes, *p21*, *Ak1*, and *Wig1*, were induced in both wild-type and *Trp53*$^{515C/515C}$ cells compared with *Trp53*-null cells. We confirmed p53R172P up-regulation of these genes by real-time RT-PCR analysis. Activation was determined by normalizing gene expression in irradiated wild-type, *Trp53*$^{515C/515C}$, and *Trp53*$^{515C/515C}$*p21*$^{-/-}$ MEFs relative to irradiated *Trp53*-null MEFs. In response to γ-radiation, wild-type p53 caused an approximate 4-fold induction of *Ak1* and *Wig1* and a robust 80-fold induction of *p21* over control cells (Fig. 6*A*). In *Trp53*$^{515C/515C}$ MEFs, p53R172P caused a 4-fold activation of *Ak1* and *Wig1* and a 10-fold activation of *p21* (Fig. 6*B*). *Trp53*$^{515C/515C}$*p21*$^{-/-}$ MEFs exhibited a 4-fold induction of *Ak1* and *Wig1*, but no change was detected in *p21* expression (Fig. 6*C*). Activation of *Ak1* and *Wig1* by p53 can inhibit cellular proliferation (29, 32, 33). Our data suggest that these factors may also play important roles in p53 tumor suppression.

Discussion

By exploiting the properties of a p53 point mutant, p53R172P, we have illustrated the importance of separate p53 activities in delaying tumor onset. Our analyses show that cooperation between p21 and apoptosis was essential for tumor suppression by p53. Mechanistically, p21 was required for cell cycle arrest and preservation of chromosomal stability. *Trp53*$^{515C/515C}$*p21*$^{-/-}$ MEFs, like *Trp53*$^{-/-}$ cells, had a defective G_1 checkpoint and developed chromosomal aberrations. Loss of *p21* also enhanced transformation of *Trp53*$^{515C/515C}$ MEFs in response to oncogenic *Ras*, whereas *Trp53*$^{515C/+}$*p21*$^{-/-}$ cells, retaining a single wild-type p53 allele, resisted *Ras*-induced transformation. These data demonstrate that a defective p53 cell cycle arrest due to the absence of *p21* imparted a proliferative advantage to cells, contributing to CIN. However, CIN was resolved in cells with an intact p53-depedendent apoptotic response. Additionally, a functional p53-dependent apoptosis pathway in *p21*$^{-/-}$ mice was associated with their tumor-free survival, whereas *Trp53*$^{515C/515C}$*p21*$^{-/-}$ and *Trp53*$^{-/-}$ mice succumbed to early onset tumorigenesis and tumors arising in these mice were characterized by CIN. Thus, p53-dependent apoptosis played an obligate role in preventing expansion of aneuploid cell populations and tumor development.

That *Trp53*$^{515C/515C}$ MEFs formed fewer foci than *Trp53*$^{-/-}$ cells in response to oncogenic *Ras* raised the possibility that p53R172P can induce replicative senescence. These data would

Table 1. p53 target genes regulated by p53R172P

Probe set	Description	FC/SE
Wild-type/*Trp53*$^{-/-}$		
96801_at	Adenylate kinase 1 (Ak1)	5.5/1.6
160127_at	Cyclin G	8.8/1.7
98067_at	Cyclin-dependent kinase inhibitor 1A (p21)	5.0/2.2
101587_at	Epoxide hydrolase 1, microsomal	13.1/0
99629_at	Etoposide-induced 2.4 mRNA	3.1/1.1
100064_at	Gap junction membrane channel protein α 1	2.5/0.1
98501_at	IL-1 receptor-like 1	2.6/0
99622_at	Kruppel-like factor 4 (gut)	2.2/0.4
99638_at	Procollagen, type XV	3.9/1.0
98110_at	Transformed mouse 3T3 cell double minute 2	3.5/0
92262_at	Wild-type p53-induced gene 1 (Wig1)	4.3/0.9
Trp53$^{C/C}$/*Trp53*$^{-/-}$		
96801_at	Adenylate kinase 1 (Ak1)	3.3/1.1
93536_at	Bcl-2 associated X protein	2.4/0.3
95423_at	Calcium-binding protein P22	2.2/0.3
98067_at	Cyclin-dependent kinase inhibitor 1A (p21)	4.8/2.1
94881_at	Cyclin-dependent kinase inhibitor 1A (p21)	9.4/3.6
92262_at	Wild-type p53-induced gene 1 (Wig1)	3.7/1.3

FC/SE, fold change/standard error.

implicate replicative senescence in tumor suppression by p53R172P.

Various studies have implicated p53 in the protection against tumor development in the context of CIN (3, 9, 34, 35). Deletion of checkpoint or DNA repair genes leads to CIN but not tumorigenesis unless p53 also is removed. Our analyses of a different cyclin-dependent kinase inhibitor suggest that loss of p53-dependent apoptosis also would enhance the tumor predisposition of *p16*^{Ink4A}-null mice. This result would implicate separate p53 functions in distinct tumor suppressor pathways.

By use of an apoptosis-deficient mouse model, our findings establish that tumor development resulting from CIN relies, specifically, upon abrogation of the p53 apoptotic pathway. In summary, we have shown that p53 cell cycle control through p21 is critical for suppressing tumorigenesis by preservation of chromosomal stability. Although p53 may serve as a gatekeeper through its apoptotic function (36), its activation of p21 fulfills its role as guardian of the genome (37).

Materials and Methods

Mice and Tumor Analysis. Generation of *Trp53*$^{515C/515C}$ mice was previously described (16). *p21*$^{-/-}$ mice were obtained from T. Jacks (Massachusetts Institute of Technology, Cambridge, MA) and were crossed with C57BL/6 mice for more than five generations until the background was at >90% C57BL/6. The background of wild-type and *Trp53*$^{-/-}$ mice was >90% C57BL/6. To detect chromosomal aberrations, lymphoma cells were isolated from affected spleens or lymph nodes by homogenization. Sarcoma cells were prepared by homogenizing tissues with trypsin for 5 min at 37°C then incubating them with 4 mg/ml collagenase D and dispase (Sigma, St. Louis, MO) for 2 h and plated in complete media. Metaphase spreads were prepared and evaluated as described (38).

Cell Culture and Apoptosis Assay. MEFs were generated from 13.5 day-old embryos. For cell cycle analysis, MEFs were treated as previously described (16). Focus-forming assays were performed as described (39) with minor modifications. After selection of MEFs with puromycin, 2,000 puromycin-resistance cells were mixed with 300,000 noninfected cells of the same genotype and plated in 100-mm dishes. Fifteen days after plating, cells were fixed and stained with crystal violet in methanol, and foci were counted. For growth curve analysis, 19,000 cells were plated in triplicate in 35-mm dishes and counted at the indicated time points. The medium was changed every 3 days. Cells were transfected with siRNAs for *p21* (40), *p16*^{Ink4a} (40) or with control siRNA (Dharmacon, Lafayette, CO) by using Lipofectamine 2000 (Invitrogen, Carlsbad, CA) according to the manufacturer's recommendations. For apoptosis assays, freshly isolated thymocytes were prepared and evaluated as previously described (16).

Immunoblot Analysis. Cell pellets were resuspended in lysis buffer (41). Forty micrograms of protein were resolved on 10% polyacrylamide gels and transferred to nitrocellulose. Membranes were incubated with anti-p53 (CM5; Novocastra Laboratories, Newcastle upon Tyne, U.K.), monoclonal anti-p21 (BD Pharmingen, San Diego, CA), anti-p16 (M-156; Santa Cruz Biotechnologies, Santa Cruz, CA), or anti-β-actin antibodies (Sigma).

Real-Time RT-PCR. MEFs were exposed to 6 Gy of γ-radiation with a ^{137}Cs source then cultured for 6 h and prepared as described (42). The primer sequences for *p21* and *Gapdh* were previously described (42). The following primer sets were also used: *Ak1*, GGAGACCATCAAGAAGCGGC and TTCGGCATTGACCTTGCG; and *Wig1*, CTACTGTAAGCTGTGCGATGCC and AGTGACTCTGAGCTTCGGCC. Expression of mRNA was normalized to expression of *Gapdh* in each reaction.

Microarray Analysis. MEFs were treated with 6 Gy of γ-radiation and harvested 6 h later. Total RNA was isolated by using an

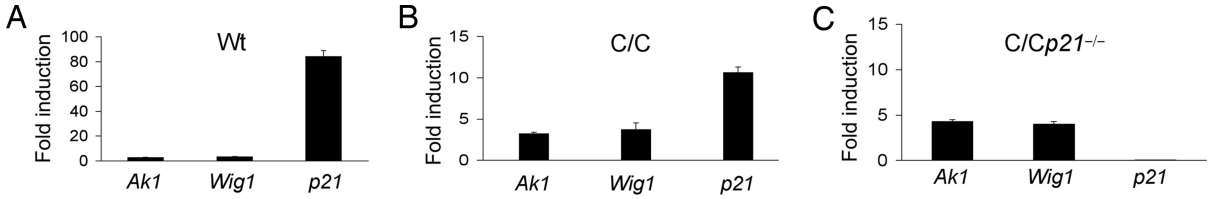

Fig. 6. Real-time RT-PCR analysis for transcriptional activation by p53R172P. Gene expression was first normalized to *Gapdh*. Fold induction was calculated as gene expression differences in irradiated (6 Gy) wild-type (*A*), *Trp53*$^{515C/515C}$ (*B*), and *Trp53*$^{515C/515Cp21-/-}$ (*C*) MEFs over that in irradiated *Trp53*-null cells. Data are depicted as the fold induction with SE from triplicate samples.

RNeasy kit (Qiagen, Valencia, CA). Ten micrograms of total RNA was used for cRNA probe preparation and hybridization onto oligonucleotide U74Av2 GeneChip arrays according to manufacturer's recommendations (Affymetrix, Santa Clara, CA). Hybridized arrays were scanned with a GeneArray Scanner (Hewlett–Packard, Palo Alto, CA). The image and intensity data were collected with Affymetrix Microarray Suite 5.0 and further analyzed by DNA-Chip Analyzer software (dChip) (43). Briefly, the scanned images were quantified with Microarray Suite 5.0 and then linearly scaled to an average expression level of 2,500 units to generate a signal intensity for each probe set. The signal intensities from the 11 or 16 probe pairs for each gene were used to determine gene expression values and differentially expressed genes with dChip. The data were first normalized against a default baseline array and expression values were calculated by using the perfect-match– mismatch model. Gene expression was considered significantly altered if all of the following conditions were met: (*i*) expression value must be called present in at least one of the paired samples for comparison; (*ii*) the difference of expression values between the paired samples was ≥ 100 to avoid the effects of unreliable low intensity; (*iii*) the ratio of expression values between the paired samples exceeds a threshold more than or equal to 1.5 or less than or equal to -1.5, with a lower confidence bound of the 90% confidence interval [lower bound of fold change (LBFC)]; (*iv*) the paired samples were significantly different, with P values ≤ 0.05 as determined by t test. The irradiation and microarray hybridization were repeated in two independent experiments, and the two independent data sets were analyzed by two strict strategies. First, the two data sets were combined to identify differentially expressed genes by using the above comparison criteria. Second, the two data sets were separately analyzed by using the same comparison criteria, and the differentially expressed genes in common between the two independent analyses were identified. The first strategy generated a single LBFC for each gene. The second strategy generated two LBFCs for each overlapping gene. The two LBFCs generated by the second strategy were averaged and a SE was obtained.

We thank Tomoo Iwakuma, Tamara Terzian, and Yasmine Valentin-Vega for guidance and helpful discussions and Sean Post for careful review of the manuscript. This study was supported by National Institutes of Health Grant CA82577 (to G. Lozano). Veterinary support, cytogenetics, and Affymetrix core facilities were supported by National Cancer Institute Cancer Center Support Grant CA16672. J.A.B. was supported by National Institutes of Health Cancer Genetics Training Grant CA009299.

1. el-Deiry WS, Tokino T, Velculescu VE, Levy DB, Parsons R, Trent JM, Lin D, Mercer WE, Kinzler KW, Vogelstein B (1993) *Cell* 75:817–825.
2. Harper JW, Adami GR, Wei N, Keyomarsi K, Elledge SJ (1993) *Cell* 75:805–816.
3. Deng C, Zhang P, Harper JW, Elledge SJ, Leder P (1995) *Cell* 82:675–684.
4. Waldman T, Kinzler KW, Vogelstein B (1995) *Cancer Res* 55:5187–5190.
5. Brugarolas J, Chandrasekaran C, Gordon JI, Beach D, Jacks T, Hannon GJ (1995) *Nature* 377:552–557.
6. Brugarolas J, Bronson RT, Jacks T (1998) *J Cell Biol* 141:503–514.
7. Franklin DS, Godfrey VL, O'Brien DA, Deng C, Xiong Y (2000) *Mol Cell Biol* 20:6147–6158.
8. Lebel M, Cardiff RD, Leder P (2001) *Cancer Res* 61:1816–1819.
9. Hollander MC, Sheikh MS, Bulavin DV, Lundgren K, Augeri-Henmueller L, Shehee R, Molinaro TA, Kim KE, Tolosa E, Ashwell JD, *et al*. (1999) *Nat Genet* 23:176–184.
10. Jeffers JR, Parganas E, Lee Y, Yang C, Wang J, Brennan J, MacLean KH, Han J, Chittenden T, Ihle JN, *et al*. (2003) *Cancer Cell* 4:321–328.
11. Knudson CM, Tung KS, Tourtellotte WG, Brown GA, Korsmeyer SJ (1995) *Science* 270:96–99.
12. Shibue T, Takeda K, Oda E, Tanaka H, Murasawa H, Takaoka A, Morishita Y, Akira S, Taniguchi T, Tanaka N (2003) *Genes Dev* 17:2233–2238.
13. Villunger A, Michalak EM, Coultas L, Mullauer F, Bock G, Ausserlechner MJ, Adams JM, Strasser A (2003) *Science* 302:1036–1038.
14. Ludwig RL, Bates S, Vousden KH (1996) *Mol Cell Biol* 16:4952–4960.
15. Rowan S, Ludwig RL, Haupt Y, Bates S, Lu X, Oren M, Vousden KH (1996) *EMBO J* 15:827–838.
16. Liu G, Parant JM, Lang G, Chau P, Chavez-Reyes A, El-Naggar AK, Multani A, Chang S, Lozano G (2004) *Nat Genet* 36:63–68.
17. Hundley JE, Koester SK, Troyer DA, Hilsenbeck SG, Subler MA, Windle JJ (1997) *Mol Cell Biol* 17:723–731.
18. Lozano G, Zambetti GP (2005) *J Pathol* 205:206–220.
19. Lowe SW, Schmitt EM, Smith SW, Osborne BA, Jacks T (1993) *Nature* 362:847–849.
20. Tanaka N, Ishihara M, Kitagawa M, Harada H, Kimura T, Matsuyama T, Lamphier MS, Aizawa S, Mak TW, Taniguchi T (1994) *Cell* 77:829–839.
21. Donehower LA, Harvey M, Slagle BL, McArthur MJ, Montgomery CA, Jr, Butel JS, Bradley A (1992) *Nature* 356:215–221.
22. Jacks T, Remington L, Williams BO, Schmitt EM, Halachmi S, Bronson RT, Weinberg RA (1994) *Curr Biol* 4:1–7.
23. Serrano M, Hannon GJ, Beach D (1993) *Nature* 366:704–707.
24. Quelle DE, Zindy F, Ashmun RA, Sherr CJ (1995) *Cell* 83:993–1000.
25. Ruas M, Peters G (1998) *Biochim Biophys Acta* 1378:F115–F177.
26. Miled C, Pontoglio M, Garbay S, Yaniv M, Weitzman JB (2005) *Cancer Res* 65:5096–5104.
27. Zhang W, Geiman DE, Shields JM, Dang DT, Mahatan CS, Kaestner KH, Biggs JR, Kraft AS, Yang VW (2000) *J Biol Chem* 275:18391–18398.
28. Varmeh-Ziaie S, Okan I, Wang Y, Magnusson KP, Warthoe P, Strauss M, Wiman KG (1997) *Oncogene* 15:2699–2704.
29. Collavin L, Lazarevic D, Utrera R, Marzinotto S, Monte M, Schneider C (1999) *Oncogene* 18:5879–5888.
30. Madden SL, Galella EA, Riley D, Bertelsen AH, Beaudry GA (1996) *Cancer Res* 56:5384–5390.
31. Hoh J, Jin S, Parrado T, Edington J, Levine AJ, Ott J (2002) *Proc Natl Acad Sci USA* 99:8467–8472.
32. Hellborg F, Qian W, Mendez-Vidal C, Asker C, Kost-Alimova M, Wilhelm M, Imreh S, Wiman KG (2001) *Oncogene* 20:5466–5474.
33. Israeli D, Tessler E, Haupt Y, Elkeles A, Wilder S, Amson R, Telerman A, Oren M (1997) *EMBO J* 16:4384–4392.
34. Bassing CH, Suh H, Ferguson DO, Chua KF, Manis J, Eckersdorff M, Gleason M, Bronson R, Lee C, Alt FW (2003) *Cell* 114:359–370.
35. Xu X, Qiao W, Linke SP, Cao L, Li WM, Furth PA, Harris CC, Deng CX (2001) *Nat Genet* 28:266–271.
36. Levine AJ (1997) *Cell* 88:323–331.
37. Lane DP (1992) *Nature* 358:15–16.
38. Hingorani SR, Wang L, Multani AS, Combs C, Deramaudt TB, Hruban RH, Rustgi AK, Chang S, Tuveson DA (2005) *Cancer Cell* 7:469–483.
39. Lang GA, Iwakuma T, Suh YA, Liu G, Rao VA, Parant JM, Valentin-Vega YA, Terzian T, Caldwell LC, Strong LC, *et al*. (2004) *Cell* 119:861–872.
40. Zou X, Ray D, Aziyu A, Christov K, Boiko AD, Gudkov AV, Kiyokawa H (2002) *Genes Dev* 16:2923–2934.
41. Kapoor M, Lozano G (1998) *Proc Natl Acad Sci USA* 95:2834–2837.
42. Iwakuma T, Parant JM, Fasulo M, Zwart E, Jacks T, de Vries A, Lozano G (2004) *Oncogene* 23:7644–7650.
43. Li C, Wong WH (2001) *Proc Natl Acad Sci USA* 98:31–36.